

Large θ_{13} from finite quantum corrections in quasi-degenerate neutrino mass spectrum

Takeshi Araki^{a)*} and Chao-Qiang Geng^{b),c)†}

^{a)}*Institute of High Energy Physics,*

Chinese Academy of Sciences, Beijing 100049, China

^{b)}*Department of Physics, National Tsing Hua University, Hsinchu 300, Taiwan*

^{c)}*Physics Division, National Center for Theoretical Sciences, Hsinchu 300, Taiwan*

Abstract

We study finite quantum corrections for several well known neutrino mixing matrices and find that it is hard to account for the large value of θ_{13} recently reported by T2K and MINOS. To nicely reproduce all experimentally favored neutrino mixing angles and masses, we propose a new neutrino mixing pattern. We also demonstrate a simple realization by slightly extending the standard model to illustrate the quantum corrections.

* araki@ihep.ac.cn

† geng@phys.nthu.edu.tw

I. INTRODUCTION

During the recent decade, neutrino oscillation experiments have provided us with valuable information on the neutrino mixing angles and masses. Despite the great progress, some of quantities in the neutrino sector have not been measured yet. In particular, one of the mixing angles, θ_{13} , has been shrouded in mystery for a long time. This angle has been believed to be very tiny compared with the other angles, and it has long been an open question whether its value is exactly zero or not. Over the years, people have attempted to indirectly extract the hint of a non-zero θ_{13} via the precision analysis of oscillation channels with a gradually improved confidence level [1–3]. Recently, the T2K [4] and MINOS [5] Collaborations have announced that they have observed some electron-like events in the $\nu_\mu \rightarrow \nu_e$ appearance channel, which is mainly sensitive to θ_{13} , with the indications of a relatively large θ_{13} : e.g., the best-fit value of θ_{13} suggested by the T2K Collaboration is around 9.7° (11.0°) for the normal (inverted) neutrino mass ordering. Moreover, at almost the same time, the possible $> 3\sigma$ evidence of a non-zero θ_{13} has been reported in a global analysis [6, 7].

In reaction to the above developments, many theoretical studies have also been performed. On one hand, in Ref. [8], the authors focus on mixing matrices which predict the vanishing θ_{13} at leading order and perturb it by introducing small corrections, so that the resultant θ_{13} can account for the T2K and MINOS indications. On the other hand, new mixing patterns with a non-zero θ_{13} at leading order are also proposed in Ref. [9]¹. In this paper, by adopting the former paradigm, we also aim at deriving a large θ_{13} in a model-dependent manner. In Ref. [12], a new theoretical scheme was proposed, in which small corrections to the neutrino mixing angles and masses are induced from finite quantum effects. In this study, we introduce relatively large corrections to investigate whether θ_{13} can largely deviate from 0° for the well known popular neutrino mixing patterns, such as tri-bimaximal (TBM) [13], bi-maximal (BM) [14], and democratic (DC) [15] mixing matrices. Furthermore, we illustrate a new (tree-level) mixing pattern, which can nicely reproduce all the experimental results after taking the finite quantum corrections into

¹ Other studies relevant to the T2K and MINOS indications can be found in Ref. [10]. For early works on a large θ_{13} , see Ref. [11].

account.

This paper is organized as follows. In Sec. II, we show a basic framework of our scheme and derive analytic expressions of the neutrino mixing angles and masses. In Sec. III, we numerically analyze the scheme for the TBM, BM, and DC mixing patterns. We also demonstrate a new mixing pattern, which works very well with our scheme. In Sec. IV, we show a simple realization of the finite quantum corrections by extending the standard model (SM) with new $SU(2)_L$ doublet and triplet scalars. We summarize the discussions in Sec. V.

II. FINITE QUANTUM CORRECTIONS

We suppose that neutrinos are Majorana particles and divide the Majorana neutrino mass matrix (M_ν) into the tree-level (M_ν^0) and one-loop (ΔM_ν) parts

$$M_\nu = M_\nu^0 + \Delta M_\nu. \quad (1)$$

The tree-level mass matrix is assumed to take the form of $M_\nu^0 = V^0 \mathcal{D}_\nu (V^0)^T$, where $\mathcal{D}_\nu = \text{Diag}(\lambda_1 e^{i\rho}, \lambda_2 e^{i\sigma}, \lambda_3)$ contains the three eigenvalues of M_ν^0 with two Majorana CP-violating phases, and V^0 stands for the tree-level mixing matrix, so that M_ν^0 is diagonalized by V^0 . We also presume the diagonal charged lepton mass matrix and the existence of a flavor symmetry which ensures $\theta_{13} = 0^\circ$ at tree level. Thus, we parametrize V^0 as

$$V^0 = \begin{pmatrix} c_{12}^0 & s_{12}^0 & 0 \\ -c_{23}^0 s_{12}^0 & c_{23}^0 c_{12}^0 & -s_{23}^0 \\ -s_{23}^0 s_{12}^0 & s_{23}^0 c_{12}^0 & c_{23}^0 \end{pmatrix}, \quad (2)$$

where $s_{ij}^0 (c_{ij}^0) = \sin \theta_{ij}^0 (\cos \theta_{ij}^0)$ with θ_{ij}^0 representing the tree-level mixing angles. For this setup, we take the following correction term:

$$\Delta M_\nu = \frac{M_\nu^0 D_\ell^2 + D_\ell^2 M_\nu^0}{v^2} \times I^{\text{loop}}, \quad (3)$$

where $D_\ell = \text{Diag}(m_e, m_\mu, m_\tau)$ denotes the diagonal charged lepton mass matrix, and $v = 174$ GeV is the vacuum-expectation-value (VEV) of the SM Higgs field. Such a correction term may emerge from a one-loop diagram. We will show a simple realization of ΔM_ν in Sec. IV. Notice that I^{loop} is a dimension-less function including the one-loop

integral. Remarkably, in this scheme, once a specific V^0 is given at tree level, the structure of ΔM_ν will be determined up to the over-all factor I^{loop} because no new Yukawa coupling is introduced.

In principle, one also needs to consider the higher-loop (finite quantum) corrections to the neutrino mixing angles and masses. However, to simplify our discussion on the generic feature of the corrections, in what follows, we will assume that these contributions are negligible. In fact, in the model presented in Sec. IV, the two-loop corrections are indeed always smaller than the one-loop correction by a factor $1/(16\pi^2)$.

We regard δM_ν as small perturbations, yielding the perturbed mixing angles:

$$\sin \theta_{13} \simeq \left| 2s_{23}^0 c_{23}^0 s_{12}^0 c_{12}^0 \frac{m_\tau^2}{v^2} \left\{ \frac{\lambda_3^2 [\lambda_1^2 + \lambda_2^2 - 2\lambda_1 \lambda_2 \cos(\rho - \sigma)]}{[\lambda_1^2 + \lambda_3^2 - 2\lambda_1 \lambda_3 \cos \rho][\lambda_2^2 + \lambda_3^2 - 2\lambda_2 \lambda_3 \cos \sigma]} \right\}^{\frac{1}{2}} I^{\text{loop}} \right|, \quad (4)$$

$$\tan \theta_{12} \simeq t_{12}^0 \left[1 + (s_{23}^0)^2 \frac{m_\tau^2}{v^2} \frac{\lambda_1^2 - \lambda_2^2}{\lambda_1^2 + \lambda_2^2 - 2\lambda_1 \lambda_2 \cos(\rho - \sigma)} I^{\text{loop}} \right], \quad (5)$$

$$\tan \theta_{23} \simeq t_{23}^0 \left\{ 1 + \frac{m_\tau^2}{v^2} \left[\frac{(s_{12}^0)^2 (\lambda_1^2 - \lambda_3^2)}{\lambda_1^2 + \lambda_3^2 - 2\lambda_1 \lambda_3 \cos \rho} + \frac{(c_{12}^0)^2 (\lambda_2^2 - \lambda_3^2)}{\lambda_2^2 + \lambda_3^2 - 2\lambda_2 \lambda_3 \cos \sigma} \right] I^{\text{loop}} \right\}, \quad (6)$$

the perturbed neutrino masses:

$$m_1 = \lambda_1 \left[1 + 2 \frac{m_\tau^2}{v^2} (s_{23}^0)^2 (s_{12}^0)^2 I^{\text{loop}} \right], \quad (7)$$

$$m_2 = \lambda_2 \left[1 + 2 \frac{m_\tau^2}{v^2} (s_{23}^0)^2 (c_{12}^0)^2 I^{\text{loop}} \right], \quad (8)$$

$$m_3 = \lambda_3 \left[1 + 2 \frac{m_\tau^2}{v^2} (c_{23}^0)^2 I^{\text{loop}} \right], \quad (9)$$

and the Jarlskog parameter [16]:

$$J_{\text{CP}} \simeq 2(s_{23}^0 c_{23}^0 s_{12}^0 c_{12}^0)^2 \frac{m_\tau^2}{v^2} \left[\frac{\lambda_2 \lambda_3 \sin \sigma}{\lambda_2^2 + \lambda_3^2 - 2\lambda_2 \lambda_3 \cos \sigma} - \frac{\lambda_1 \lambda_3 \sin \rho}{\lambda_1^2 + \lambda_3^2 - 2\lambda_1 \lambda_3 \cos \rho} \right] I^{\text{loop}}, \quad (10)$$

where we have ignored the muon and electron masses. In contrast, there are no corrections to ρ and σ , which are Majorana CP-violating phases defined below Eq. (1), up to this order.

Here, we would emphasize two important features of the perturbed mixing angles, which will be crucial when we discuss the results of numerical calculations in the next section. (i) As found in the studies of renormalization-group equations [17], corrections to the mixing angles can be enhanced due to the degeneracy among three neutrino masses. Particularly, in view of $\Delta m_{21}^2 \ll \Delta m_{31}^2$ and $\lambda_i \simeq m_i$, we can conjecture that θ_{12} is the most

sensitive one to this enhancement [12]. However, because the strength of the enhancement depends also on the Majorana CP-violating phases as well as the differences between λ_i and m_i , the enhancement is not always strong even in the case of the quasi-degenerate neutrino mass spectrum. (ii) Relative signs between the tree-level mixing angles and their corrections can approximately be determined by the sign of I^{loop} and the neutrino mass ordering in the sense of $\lambda_i \simeq m_i$. In fact, from Eqs. (5) and (6), one can immediately read out the following behaviors:

- $I^{\text{loop}} > (<)0$ leads to $\theta_{12} < (>)\theta_{12}^0$,
- NO with $I^{\text{loop}} > (<)0$ and IO with $I^{\text{loop}} < (>)0$ yield $\theta_{23} < (>)\theta_{23}^0$,

where NO (IO) denotes the normal (inverted) neutrino mass ordering.

III. NUMERICAL CALCULATIONS

A. Input parameters

Instead of a perturbative method, we numerically diagonalize the full neutrino mass matrix of Eq. (1) and compute the neutrino mixing angles and masses. From the recent global analysis [2] of the neutrino oscillation data, we refer to the following best-fit values and 1σ (3σ) error bounds:

$$\begin{aligned} \Delta m_{21}^2 &= \left(7.59_{-0.18(0.50)}^{+0.20(0.60)}\right) \times 10^{-5} \text{ eV}^2, \\ \Delta m_{31}^2 &= \begin{cases} + \left(2.45_{-0.09(0.27)}^{+0.09(0.28)}\right) \times 10^{-3} \text{ eV}^2 & \text{for Normal Ordering (NO)} \\ - \left(2.34_{-0.09(0.26)}^{+0.10(0.30)}\right) \times 10^{-3} \text{ eV}^2 & \text{for Inverted Ordering (IO)} \end{cases}, \\ \theta_{12} &= \left(34.0_{-1.0(2.7)}^{+1.0(2.9)}\right)^\circ, \quad \theta_{23} = \begin{cases} \left(45.6_{-3.5(7.0)}^{+3.4(7.5)}\right)^\circ \\ \left(46.1_{-3.4(7.5)}^{+3.5(7.0)}\right)^\circ \end{cases}, \quad \theta_{13} = \begin{cases} \left(5.7_{-2.1(--)}^{+2.2(5.1)}\right)^\circ \\ \left(6.5_{-2.1(--)}^{+2.0(4.9)}\right)^\circ \end{cases}, \end{aligned} \quad (11)$$

where the upper and lower values of Δm_{31}^2 , θ_{23} , and θ_{13} correspond to the NO and IO, respectively. In the following calculations, unless otherwise stated, we impose the 3σ constraints on Δm_{21}^2 , Δm_{31}^2 , and θ_{12} to examine θ_{13} and θ_{23} as well as J_{CP} . Besides, we use the charged lepton masses at the electroweak scale as [18]

$$m_e = 0.486 \text{ MeV}, \quad m_\mu = 102.718 \text{ MeV}, \quad m_\tau = 1746.24 \text{ MeV}. \quad (12)$$

We vary the Majorana phases (ρ and σ) within 0° to 360° and λ_i to fit the two mass-squared differences. Moreover, in order to enhance the corrections to the mixing angles, we consider the quasi-degenerate neutrino mass spectrum and fix the heaviest neutrino mass as 0.2 eV, i.e., $m_{3(2)} = 0.2$ eV in the case of the NO (IO). In this case, $|I^{\text{loop}}| \simeq 100$ is needed to realize $\theta_{13} \simeq 10^\circ$. Here, we vary I^{loop} within -125 to 125 , so that a maximal value of $\theta_{13} \simeq 13^\circ$ can be produced. We note that almost the same results can be obtained for the different choices of $m_{3(2)}$ and I^{loop} , e.g., $m_{3(2)} = 0.3$ eV with $|I^{\text{loop}}| < 55$ or $m_{3(2)} = 0.4$ eV with $|I^{\text{loop}}| < 30$.

B. Tri-bimaximal (TBM) mixing

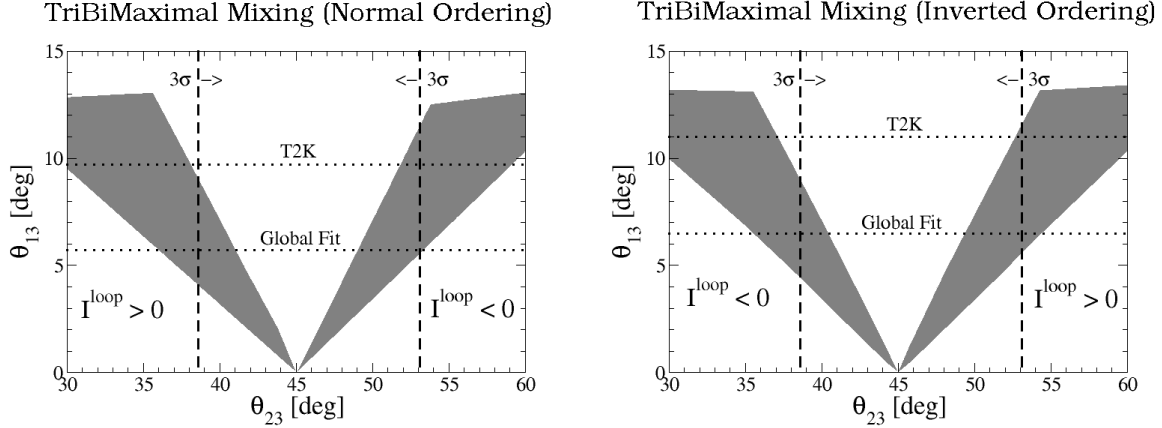


FIG. 1: θ_{13} as functions of θ_{23} for the normal ordering (NO) and inverted ordering (IO) at the left and right panels, respectively, with the tri-bimaximal (TBM) tree-level mixing matrix, where the horizontal dotted lines display the best-fit values of θ_{13} from the T2K experiment [4] and Eq. (11), while the vertical dashed lines express the 3σ upper and lower bounds of θ_{23} from Eq. (11).

Let us employ the TBM mixing

$$V_{\text{TB}}^0 = \frac{1}{\sqrt{6}} \begin{pmatrix} 2 & \sqrt{2} & 0 \\ -1 & \sqrt{2} & -\sqrt{3} \\ -1 & \sqrt{2} & \sqrt{3} \end{pmatrix} \quad (13)$$

as the tree-level mixing matrix. Namely, we substitute $\theta_{12}^0 \simeq 35.26^\circ$ and $\theta_{23}^0 = 45^\circ$ in Eq. (2). In Fig. 1, we compute θ_{13} as functions of θ_{23} for the NO (left panel) and IO (right

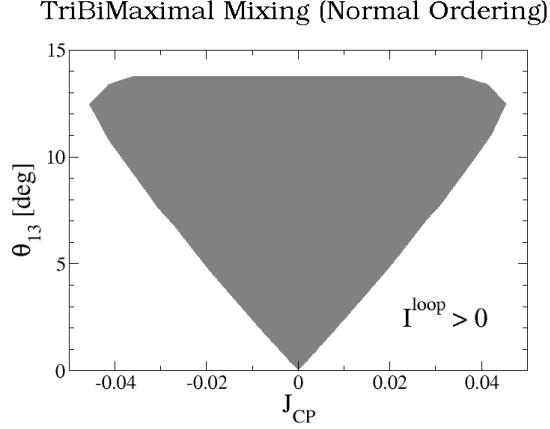


FIG. 2: θ_{13} as a function of J_{CP} for the normal ordering (NO) with $I^{\text{loop}} > 0$ in the case where the tree-level mixing matrix is the tri-bimaximal (TBM) one.

panel), respectively. As can be seen, θ_{13} can largely deviate from 0° and it can even be $10^\circ \sim 11^\circ$, favored by the T2K experiment [4]. However, such a large θ_{13} simultaneously leads to a large deviation of θ_{23} from 45° . For instance, if we demand the 3σ constraint of θ_{23} in Eq. (11), θ_{13} can maximally be 9.0° (11.5°) and 11.2° (9.0°) for $I^{\text{loop}} > 0$ and $I^{\text{loop}} < 0$, respectively, in the case of the NO (IO), but these values correspond to the edges of 3σ upper and lower bounds of θ_{23} . Therefore, $\theta_{13} \simeq 10^\circ$ cannot be accompanied with a nearly maximal θ_{23} , which is favored by the neutrino oscillation data, in the TBM mixing case. In Fig. 2, we also plot θ_{13} as a function of J_{CP} for only the NO with $I^{\text{loop}} > 0$ case and find that J_{CP} can be of $\mathcal{O}(0.01)$. In this plane, the sign of I^{loop} and the neutrino mass ordering do not make a large difference to the shape of allowed regions. Note that the $I^{\text{loop}} < 0$ case is excluded at the 1σ level due to $\theta_{12} > 35.26^\circ$, mentioned at the end of Sec. II.

C. Bi-maximal (BM) mixing

We use the BM mixing

$$V_{\text{BM}}^0 = \frac{1}{2} \begin{pmatrix} \sqrt{2} & \sqrt{2} & 0 \\ -1 & 1 & -\sqrt{2} \\ -1 & 1 & \sqrt{2} \end{pmatrix} \quad (14)$$

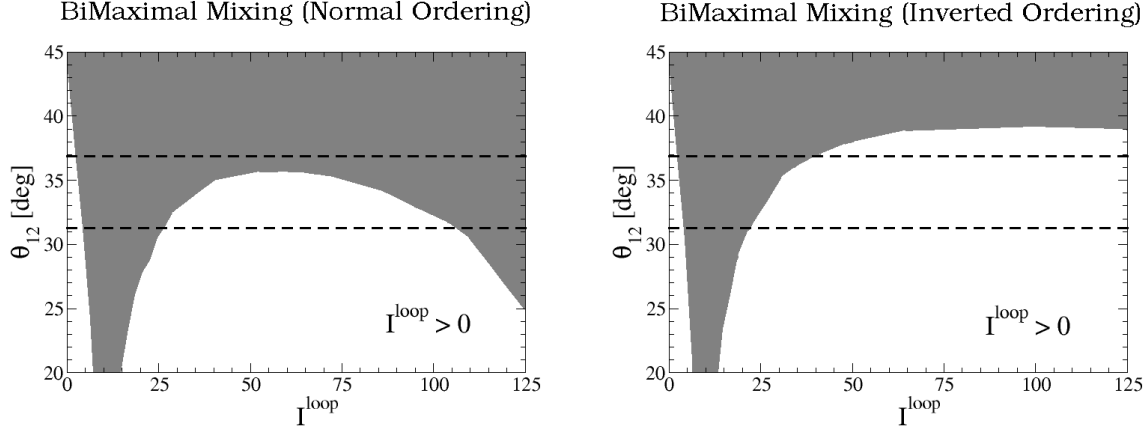


FIG. 3: θ_{12} as functions of $I^{\text{loop}} > 0$ for the normal ordering (NO) and inverted ordering (IO) at the left and right panels, respectively, with the bi-maximal (BM) tree-level mixing matrix, where the dashed lines display the 3σ upper and lower bounds of θ_{12} from Eq. (11).

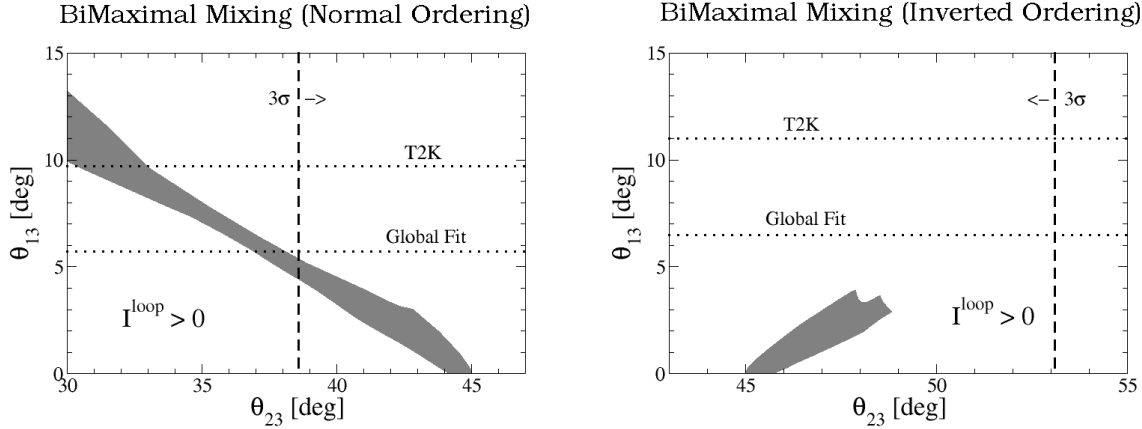


FIG. 4: Legend is the same as Fig. 1 except that the tree-level mixing matrix is the bi-maximal (BM) one with $I^{\text{loop}} > 0$.

as the tree-level mixing matrix with $\theta_{12}^0 = \theta_{23}^0 = 45^\circ$ for Eq. (2). In the case of $I^{\text{loop}} < 0$, this tree-level mixing results in $\theta_{12} > 45^\circ$, and it is clearly inconsistent with experiments. Furthermore, even in the case of $I^{\text{loop}} > 0$, θ_{12} cannot always account for the 3σ upper bound ($\theta_{12} < 36.9^\circ$), so that the allowed regions are restricted in comparison with those of the TBM case. To illustrate the behavior of θ_{12} , in Fig. 3, we calculate θ_{12} as a function of I^{loop} with respect to only the 3σ constraints of Δm_{21}^2 and Δm_{31}^2 . As one can see,

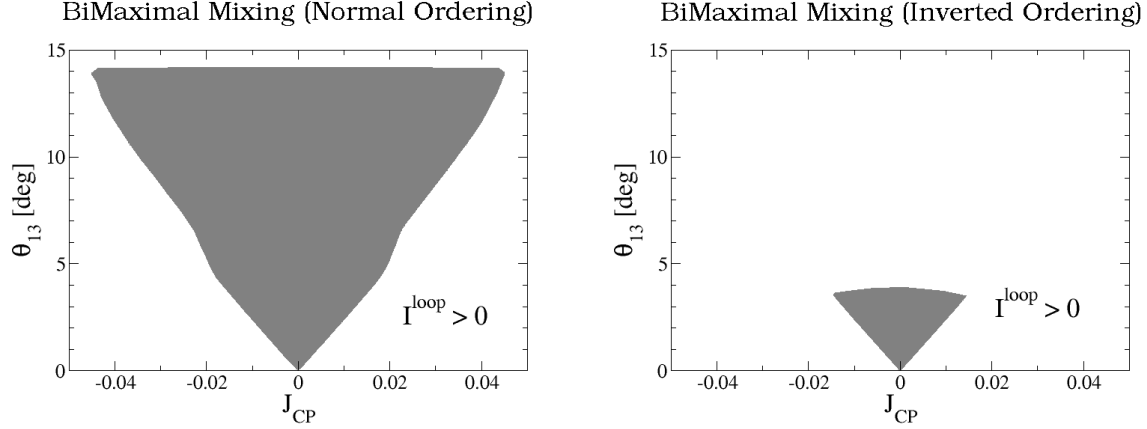


FIG. 5: θ_{13} as functions of J_{CP} for the normal ordering (NO) and inverted ordering (IO) at the left and right panels, respectively, with $I^{\text{loop}} > 0$ in the case where the tree-level mixing matrix is the bi-maximal (BM) one.

the corrections of θ_{12} are maximally enhanced around $I^{\text{loop}} \simeq 10$, but the enhancement becomes weaker as I^{loop} increases. Especially, in the IO case, θ_{12} gets always away from the 3σ range after $I^{\text{loop}} \simeq 40$. In turn, we restore the 3σ constraint of θ_{12} and plot θ_{13} as functions of θ_{23} and J_{CP} in Figs. 4 and 5, respectively. In the case of the NO, θ_{13} can maximally be 5.3° at the 3σ lower bound of θ_{23} , while it can be 4.0° at $\theta_{23} \simeq 48^\circ$ (and $\theta_{12} \simeq 36.9^\circ$) in the IO case. Hence, we conclude that the BM mixing case cannot explain $\theta_{13} \simeq 10^\circ$, favored by the T2K experiment, while keeping the other angles within experimentally favored ranges. Also, the allowed region of J_{CP} is strictly limited in the IO case.

D. Democratic (DC) mixing

We take the DC mixing

$$V_{\text{DC}}^0 = \frac{1}{\sqrt{6}} \begin{pmatrix} \sqrt{3} & \sqrt{3} & 0 \\ -1 & 1 & -2 \\ -\sqrt{2} & \sqrt{2} & \sqrt{2} \end{pmatrix} \quad (15)$$

as the tree-level mixing matrix with $\theta_{12}^0 = 45^\circ$ and $\theta_{23}^0 \simeq 54.74^\circ$ for Eq. (2). In the case of $I^{\text{loop}} < 0$, this tree-level mixing works out $\theta_{12} > 45^\circ$, and it is clearly inconsistent with

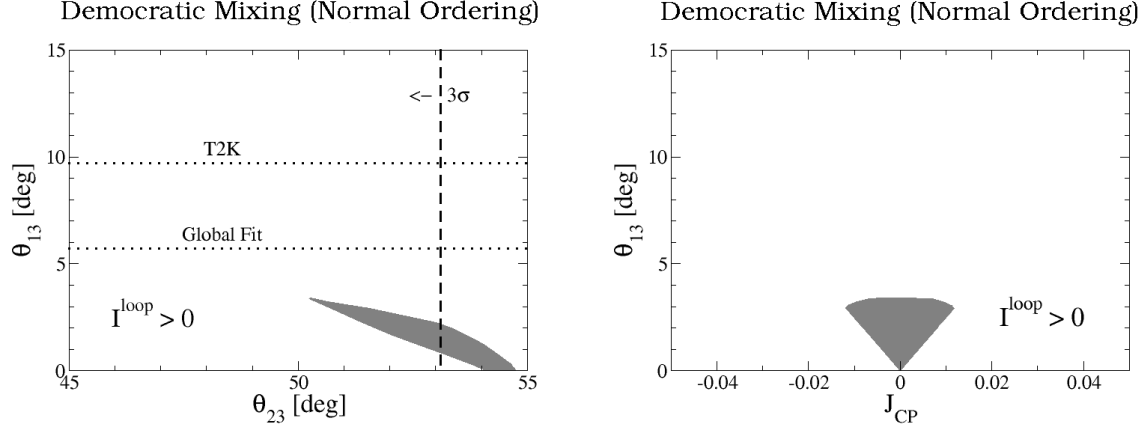


FIG. 6: Legend is the same as Figs. 1 and 2 but with the democratic (DC) tree-level mixing matrix and $I^{\text{loop}} > 0$.

experiments. Similarly, the IO with $I^{\text{loop}} > 0$ case results in $\theta_{23} > 54.74^\circ$, and this case is obviously disfavored by experiments, too. Thus, the only possible combination is the NO with $I^{\text{loop}} > 0$ one. Even in this case, however, the allowed regions are strictly constrained by θ_{12} , like the BM case. From Fig. 6, one can read off that the maximum deviation of θ_{13} from 0° is only 3.4° at $\theta_{23} \simeq 50^\circ$ (and $\theta_{12} \simeq 36.9^\circ$), which indicates that the DC mixing is incompatible with our scheme to reproduce the large value of θ_{13} .

E. New mixing

From results we have obtained so far, we can read out several tendencies of our scheme: (i) θ_{13} can largely deviate from 0° with a relatively large I^{loop} , (ii) the large deviation of θ_{13} is always accompanied with a large deviation of θ_{23} from its initial value, and (iii) in the large I^{loop} region, θ_{12} cannot always drastically depart from its initial value. Due to these tendencies, we invent a new mixing pattern

$$V_{\text{new}}^0 = \frac{1}{3} \begin{pmatrix} \sqrt{6} & \sqrt{3} & 0 \\ -1 & \sqrt{2} & -\sqrt{6} \\ -\sqrt{2} & 2 & \sqrt{3} \end{pmatrix}, \quad (16)$$

which predicts $\theta_{12}^0 = 35.26^\circ$, $\theta_{23}^0 = 54.74^\circ$, and $\theta_{13}^0 = 0^\circ$ at tree level. We will demonstrate that this mixing matrix can nicely reproduce all the experimental results after taking

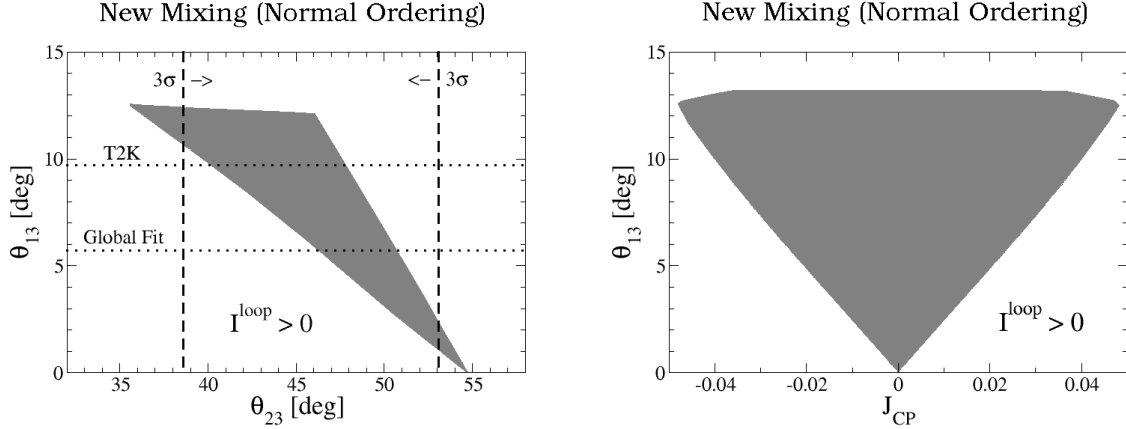


FIG. 7: θ_{13} as functions of θ_{23} (left panel) and J_{CP} (right panel) for the normal ordering (NO) with $I^{\text{loop}} > 0$ in the case where the tree-level mixing matrix takes the form of Eq. (16). Legends of the lines are the same as Fig. 1.

account of the finite quantum corrections. However, for the NO with $I^{\text{loop}} < 0$ and IO with $I^{\text{loop}} > 0$, the mixing matrix in Eq. (16) results in $\theta_{23} > 54.74^\circ$. Hence, we will concentrate on the cases of the NO with $I^{\text{loop}} > 0$ and IO with $I^{\text{loop}} < 0$. In Fig. 7, we plot θ_{13} as functions of θ_{23} (left panel) and J_{CP} (right panel) for the NO one. Figures for the IO case are almost the same as Fig. 7. The allowed regions in the figures are compatible with experiments very well. Consequently, θ_{13} can account for the best-fit values of the T2K experiment and Eq. (11) around the best-fit value of θ_{23} . Moreover, we compute χ^2 for Δm_{21}^2 , Δm_{31}^2 , θ_{12} , θ_{23} , and θ_{13} based on the best-fit values and 1σ errors given in both Eq. (11) and Ref. [6]:

$$\begin{aligned} \Delta m_{21}^2 &= \left(7.58_{-0.26}^{+0.22}\right) \times 10^{-5} \text{ eV}^2, & |\Delta m_{31}^2| &= \left(2.35_{-0.09}^{+0.12}\right) \times 10^{-3} \text{ eV}^2, \\ \theta_{12} &= (34.0 \pm 1.0)^\circ, & \theta_{23} &= \left(40.4_{-1.8}^{+4.6}\right)^\circ, & \theta_{13} &= \left(9.1_{-1.4}^{+1.2}\right)^\circ, \end{aligned} \quad (17)$$

in which new T2K and MINOS results are involved. At the point where χ^2 turns out to be minimum, based on Eqs. (11) and (17) we obtain the results as follows:

$$\begin{aligned} \Delta m_{21}^2 &= 7.59 \times 10^{-5} \text{ eV}^2, & \Delta m_{31}^2 &= 2.47 \times 10^{-3} \text{ eV}^2, \\ \theta_{12} &= 34.1^\circ, & \theta_{23} &= 46.6^\circ, & \theta_{13} &= 6.3^\circ \end{aligned} \quad (18)$$

and

$$\Delta m_{21}^2 = 7.61 \times 10^{-5} \text{ eV}^2, \quad \Delta m_{31}^2 = 2.36 \times 10^{-3} \text{ eV}^2,$$

$$\theta_{12} = 33.8^\circ, \quad \theta_{23} = 41.3^\circ, \quad \theta_{13} = 9.1^\circ \quad (19)$$

for the NO, and

$$\begin{aligned} \Delta m_{21}^2 &= 7.63 \times 10^{-5} \text{ eV}^2, \quad \Delta m_{31}^2 = 2.33 \times 10^{-3} \text{ eV}^2, \\ \theta_{12} &= 34.7^\circ, \quad \theta_{23} = 45.5^\circ, \quad \theta_{13} = 6.8^\circ \end{aligned} \quad (20)$$

and

$$\begin{aligned} \Delta m_{21}^2 &= 7.62 \times 10^{-5} \text{ eV}^2, \quad \Delta m_{31}^2 = 2.35 \times 10^{-3} \text{ eV}^2, \\ \theta_{12} &= 34.3^\circ, \quad \theta_{23} = 41.2^\circ, \quad \theta_{13} = 9.4^\circ \end{aligned} \quad (21)$$

for the IO, respectively.

F. Summary of numerical calculations

In Table I, we summarize the allowed ranges of θ_{13} , θ_{23} , and J_{CP} with respect to not only the 3σ constraints of Δm_{31}^2 , Δm_{21}^2 , and θ_{12} from Eq. (11) but also that of θ_{23} . Note that the maximum values of θ_{13} and J_{CP} in the new mixing case correspond to both the 3σ edges of θ_{23} and the assumed maximal value of I^{loop} , so that they can be larger with an even more larger value of I^{loop} .

IV. SIMPLE REALIZATION OF FINITE QUANTUM CORRECTIONS

We show a simple realization of the finite quantum correction assumed in Eq. (3). We consider a two-Higgs-doublet-extension of the SM and further introduce an $SU(2)_L$ triplet scalar, Δ , which possesses $Y = 2$. Besides, we impose a Z_4 symmetry in order to avoid the dangerous flavor changing neutral currents in the quark sector. The particle content with charge assignments of the model is summarized in Table II. The Yukawa Lagrangian and scalar potential are given by

$$\mathcal{L}_y = Y_d \bar{Q}_L H_d d_R + Y_u \bar{Q}_L (i\sigma_2 H_u^*) u_R + Y_\ell \bar{L}_L H_d \ell_R + Y_\Delta L_L^T C (i\sigma_2 \Delta) L_L + h.c. , \quad (22)$$

where σ_2 is the Pauli matrix and C stands for the charge conjugation matrix, and

$$V = n_u^2 H_u^\dagger H_u + n_d^2 H_d^\dagger H_d + n_\Delta^2 \text{Tr}[\Delta \Delta^\dagger] + \mu \left[H_u^T (i\sigma_2 \Delta^\dagger) H_d + h.c. \right]$$

Mixing	Ordering	I^{loop}	θ_{13}	θ_{23}	J_{CP}
TBM	NO	+	$0.0^\circ \sim \underline{9.0^\circ}$	$\underline{38.6^\circ} \sim 45.0^\circ$	$0.0 \pm \underline{0.033}$
		−	$0.0^\circ \sim \overline{11.2^\circ}$	$45.0^\circ \sim \overline{53.1^\circ}$	$0.0 \pm \overline{0.041}$
	IO	+	$0.0^\circ \sim \overline{11.5^\circ}$	$45.0^\circ \sim \overline{53.1^\circ}$	$0.0 \pm \overline{0.042}$
		−	$0.0^\circ \sim \underline{9.0^\circ}$	$\underline{38.6^\circ} \sim 45.0^\circ$	$0.0 \pm \underline{0.033}$
BM	NO	+	$0.0^\circ \sim \underline{5.3^\circ}$	$\underline{38.6^\circ} \sim 45.0^\circ$	$0.0 \pm \underline{0.018}$
		−	excluded		
	IO	+	$0.0^\circ \sim \langle 3.9^\circ \rangle$	$45.0^\circ \sim 48.9^\circ$	0.0 ± 0.014
		−	excluded		
DC	NO	+	$\overline{0.9^\circ} \sim \langle 3.4^\circ \rangle$	$50.2^\circ \sim \overline{53.1^\circ}$	0.0 ± 0.012
		−	excluded		
	IO	+	excluded		
		−	excluded		
New	NO	+	$\overline{1.1^\circ} \sim 12.5^\circ$	$\underline{38.6^\circ} \sim \overline{53.1^\circ}$	0.0 ± 0.047
		−	excluded		
	IO	+	excluded		
		+	$\overline{1.1^\circ} \sim 12.5^\circ$	$\underline{38.6^\circ} \sim \overline{53.1^\circ}$	0.0 ± 0.047

TABLE I: The allowed ranges of θ_{13} , θ_{23} , and J_{CP} with respect to the 3σ constraints of Δm_{31}^2 , Δm_{21}^2 , and θ_{12} given in Eq. (11), where the ranges of θ_{23} are also restricted to be within the 3σ bounds. The under and over lines to the values represent the lower and upper edges of θ_{23} , respectively, while the values surrounded by $\langle \rangle$ are limited by the 3σ upper bound of θ_{12} .

$$\begin{aligned}
& +\lambda_1 |H_u^\dagger H_u|^2 + \lambda_2 |H_d^\dagger H_d|^2 + \lambda_3 \left[(H_u^\dagger H_d)^2 + h.c. \right] + \lambda_4 (H_u^\dagger H_d)(H_d^\dagger H_u) \\
& +\lambda_5 (H_u^\dagger H_u)(H_d^\dagger H_d) + \lambda_6 \left(\text{Tr}[\Delta\Delta^\dagger] \right)^2 + \lambda_7 \text{Tr}(\Delta\Delta^\dagger\Delta\Delta^\dagger) \\
& +\lambda_8 (H_u^\dagger H_u)\text{Tr}[\Delta\Delta^\dagger] + \lambda_9 (H_d^\dagger H_d)\text{Tr}[\Delta\Delta^\dagger] \\
& +\lambda_{10} H_u^\dagger \Delta\Delta^\dagger H_u + \lambda_{11} H_d^\dagger \Delta\Delta^\dagger H_d,
\end{aligned} \tag{23}$$

	Q_L	d_R	u_R	L_L	ℓ_R	H_u	H_d	Δ
$SU(2)_L$	2	1	1	2	1	2	2	3
$U(1)_Y$	1/3	-2/3	4/3	-1	-2	1	1	2
Z_4	0	1	1	0	1	1	3	0

TABLE II: The particle content with charge assignments of the model.

respectively, with the following conventions of the scalars:

$$H_{u,d} = \begin{pmatrix} \phi_{u,d}^+ \\ h_{u,d} + i\eta_{u,d} \end{pmatrix}, \quad \Delta = \begin{pmatrix} \frac{1}{\sqrt{2}}\Delta^+ & \Delta^{++} \\ \Delta^0 + i\delta & -\frac{1}{\sqrt{2}}\Delta^+ \end{pmatrix}. \quad (24)$$

In the potential, all the couplings are chosen to be real without loss of generality.

Although there are many parameters in the potential, not all of them are indispensable for the following discussions. Hence, just for simplicity, we turn off $\lambda_4 \cdots \lambda_{11}$ from now on. By solving the stationary conditions for $h_{u,d}$ and Δ^0 , we arrive at the VEV configurations:

$$v_u^2 = \frac{\mu v_\Delta \tan^{-1} \beta - n_u^2}{2\lambda_1 + 2\lambda_3 \tan^{-2} \beta}, \quad v_d^2 = \frac{\mu v_\Delta \tan \beta - n_d^2}{2\lambda_2 + 2\lambda_3 \tan^2 \beta}, \quad v_\Delta = \frac{\mu v_u v_d}{n_\Delta^2}, \quad (25)$$

where $\tan \beta = v_u/v_d$.

As we shall explain later, v_Δ is responsible for the tree-level neutrino masses and thus, the smallness of neutrino masses originates in that of μ/n_Δ^2 . In general, both μ and n_Δ can take extremely large values. Nevertheless, in order to make the discussion more simple, we restrict ourselves to the case of $n_\Delta \gg v_{u,d} \gg \mu \gg v_\Delta$. In this limit, the mass eigenstates of singly-charged scalars are given by

$$P^\pm = \cos \beta \phi_u^\pm - \sin \beta \phi_d^\pm, \quad G^\pm = \sin \beta \phi_u^\pm + \cos \beta \phi_d^\pm \quad (26)$$

with their masses $M_{P^\pm}^2 = 2\lambda_3 v^2$ and $M_{G^\pm}^2 = 0$, where $v^2 = v_u^2 + v_d^2 = (174 \text{ GeV})^2$. Note that the mass scales of $\Delta^{\pm\pm}$, Δ^\pm , Δ^0 , and δ are mutually described by n_Δ .

The charged fermions acquire their masses through the Higgs mechanism, given by

$$M_d = Y_d v_d, \quad M_u = Y_u v_u, \quad M_\ell = Y_\ell v_d, \quad (27)$$

while Majorana neutrino masses result from the $Y_\Delta L^T \Delta L$ term after Δ^0 develops a VEV [19], given by

$$M_\nu^0 = Y_\Delta v_\Delta = Y_\Delta \frac{\mu v_u v_d}{n_\Delta^2}. \quad (28)$$

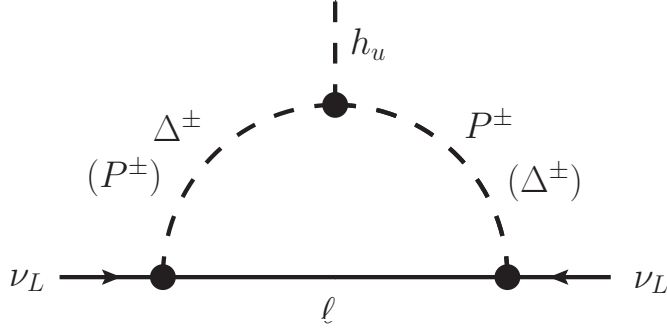


FIG. 8: A one-loop neutrino mass operator.

Furthermore, from $Y_\Delta L^T \Delta L$, $Y_\ell \bar{L} H_d \ell$, and $\mu H_u^T \Delta^\dagger H_d$ terms, a one-loop neutrino mass operator can be induced via the diagram depicted in Fig. 8. If we require $\tan \beta \gg 1$, the one-loop mass matrix can be written as

$$\delta M_\nu \simeq \frac{M_\nu^0 D_\ell^2 + D_\ell^2 M_\nu^0}{v^2} \times \left(-\frac{\tan^2 \beta}{16\pi^2} \frac{1}{1 - M_{P^\pm}^2/M_{\Delta^\pm}^2} \ln \frac{M_{P^\pm}^2}{M_{\Delta^\pm}^2} \right), \quad (29)$$

where we have assumed $\sin \beta = 1$. For example, by taking $M_{P^\pm} = 10^2$ GeV, $M_{\Delta^\pm} = 10^3$ GeV (or 10^5 GeV), and $\tan \beta = 32$ (or 38), we obtain $I^{\text{loop}} \simeq 30$ (or 126) with $\mu \simeq 10^{-6}$ GeV (or 10^{-2} GeV).

V. SUMMARY

We have applied the scheme of finite quantum corrections to the TBM, BM, and DC mixing patterns and systematically investigated how large θ_{13} can depart from 0° . We have found that (i) θ_{13} can largely deviate from 0° with a relatively large I^{loop} , (ii) the large deviation of θ_{13} is always accompanied with a large deviation of θ_{23} from its initial value, and (iii) in the large I^{loop} region, θ_{12} cannot always drastically depart from its initial value. Because of these features, unfortunately, all the TBM, BM, and DC patterns cannot reproduce the experimentally favored mixing angles and masses after taking the finite quantum corrections into account. Instead of these well known mixing patterns, we have shown an example of a new tree-level mixing matrix, which works very well with our scheme. We have also proposed a simple realization of the finite quantum corrections by introducing new $SU(2)_L$ doublet and triplet scalars with a Z_4 symmetry.

Finally, we remark that the above conclusions may be valid only for the finite quantum corrections introduced in Eq. (3). Different types² of the corrections may result in different conclusions. Nevertheless, we do not go into more detail on this possibility since it goes beyond the scope of this paper.

Acknowledgments

We are grateful to Z.Z. Xing for useful discussions and the early stage of this work. The work of T.A. was supported in part by the National Natural Science Foundation of China under Grant No. 10875131. The work of C.Q.G. was partially supported by the National Science Council under Grant No. NSC-98-2112-M-007-008-MY3 and National Center of Theoretical Science.

-
- [1] G. L. Fogli, E. Lisi, A. Marrone, A. Palazzo, and A. M. Rotunno, Phys. Rev. Lett. **101**, 141801 (2008); in *Talk given at 13th International Workshop on Neutrino Telescopes*, arXiv:0905.3549 [hep-ph].
 - [2] T. Schwetz, M. A. Tortola, and J. W. F. Valle, New J. Phys. **10**, 113011 (2008); New J. Phys. **13**, 063004 (2011).
 - [3] M. C. Gonzalez-Garcia, M. Maltoni, and J. Salvado, JHEP **1004**, 056 (2010).
 - [4] The T2K Collaboration, Phys. Rev. Lett. **107**, 041801 (2011).
 - [5] The MINOS Collaboration, arXiv:1108.0015 [hep-ex].
 - [6] G. L. Fogli, E. Lisi, A. Marrone, A. Palazzo, and A. M. Rotunno, arXiv:1106.6028 [hep-ph].
 - [7] T. Schwetz, M. A. Tortola, and J. W. F. Valle, arXiv:1108.1376 [hep-ph].
 - [8] Z. Z. Xing, arXiv:1106.3244 [hep-ph]; E. Ma and D. Wegman, Phys. Rev. Lett. **107**, 061803 (2011); X. G. He and A. Zee, arXiv:1106.4359 [hep-ph]; S. Zhou, arXiv:1106.4808 [hep-ph]; T. Araki, Phys. Rev. D **84**, 037301 (2011); N. Haba and R. Takahashi, Phys. Lett. B **702**, 388 (2011); D. Meloni, arXiv:1107.0221 [hep-ph]; W. Chao and Y. J. Zheng, arXiv:1107.0738 [hep-ph]; S. Dev, S. Gupta, and R. R. Gautam, arXiv:1107.1125 [hep-ph].

² In Ref. [12], two-loop finite quantum corrections are also discussed.

- [9] S. Morisi, K. M. Patel, and E. Peinado, arXiv:1107.0696 [hep-ph]; H. Zhang and S. Zhou, arXiv:1107.1097 [hep-ph]; R. D. A. Toorop, F. Feruglio, and C. Hagedorn, arXiv:1107.3486 [hep-ph]; W. Rodejohann, H. Zhang, and S. Zhou, arXiv:1107.3970 [hep-ph].
- [10] S. N. Gninenko, arXiv:1107.0279 [hep-ph]; X. Chu, M. Dhen, and T. Hambye, arXiv:1107.1589 [hep-ph]; P. S. B. Dev, R. N. Mohapatra, and M. Severson, arXiv:1107.2378 [hep-ph].
- [11] S. F. King, Phys. Lett. B **675**, 347 (2009); S. Goswami, S. T. Petcov, S. Ray, and W. Rodejohann, Phys. Rev. D **80**, 053013 (2009); G. Altarelli, F. Feruglio, and L. Merlo, JHEP **0905**, 020 (2009); Z. Z. Xing, Phys. Lett. B **696**, 232 (2011); Y. Shimizu, M. Tanimoto, and A. Watanabe, Prog. Theor. Phys. **126**, 81 (2011); J. A. Escobar, arXiv:1102.1649 [hep-ph]; C. Liu, Nucl. Phys. Proc. Suppl. **175-176**, 233 (2008) [arXiv:1107.1460 [hep-ph]].
- [12] T. Araki, C. Q. Geng, and Z. Z. Xing, Phys. Lett. B **699**, 276 (2011).
- [13] P. F. Harrison, D. H. Perkins, and W. G. Scott, Phys. Lett. B **530**, 167 (2002); Z. Z. Xing, Phys. Lett. B **533**, 85 (2002); P. F. Harrison and W. G. Scott, Phys. Lett. B **535**, 163 (2002).
- [14] F. Vissani, hep-ph/9708483; V. D. Barger, S. Pakvasa, T. J. Weiler, and K. Whisnant, Phys. Lett. B **437**, 107 (1998); H. Fritzsch and Z. Z. Xing, Phys. Lett. B **440**, 313 (1998).
- [15] H. Fritzsch and Z. Z. Xing, Phys. Lett. B **372**, 265 (1996); Phys. Lett. B **440**, 313 (1998); Phys. Rev. D **61**, 073016 (2000); Z. Z. Xing, Phys. Lett. B **696**, 232 (2011).
- [16] C. Jarlskog, Phys. Rev. Lett. **55**, 1039 (1985).
- [17] See, e.g., J. A. Casas, J. R. Espinosa, A. Ibarra, and I. Navarro, Nucl. Phys. B **573**, 652 (2000); S. Antusch, J. Kersten, M. Lindner, and M. Ratz, Nucl. Phys. B **674**, 401 (2003).
- [18] Z. Z. Xing, H. Zhang, and S. Zhou, Phys. Rev. D **77**, 113016 (2008).
- [19] W. Konetschny and W. Kummer, Phys. Lett. B **70**, 433 (1977); J. Schechter and J. W. F. Valle, Phys. Rev. D **22**, 2227 (1980); T. P. Cheng and L. F. Li, Phys. Rev. D **22**, 2860 (1980); G. Lazarides, Q. Shafi, and C. Wetterich, Nucl. Phys. B **181**, 287 (1981); G. B. Gelmini and M. Roncadelli, Phys. Lett. B **99**, 411 (1981).